Journal of Organometallic Chemistry 874 (2018) 74–82

Contents lists available at ScienceDirect

Journal of Organometallic Chemistry

journal homepage: www.elsevier.com/locate/jorganchem

Trichlorostannyl complexes of Ruthenium(II): Synthesis, structure, reactivity and computational studies

Nuria Álvarez-Pazos [a], Gabriele Albertin [b], Stefano Antoniutti [b], Jorge Bravo [a], Soledad García-Fontán [a, *], J.M. Hermida-Ramón [c], Gianluigi Zanardo [b]

[a] Departamento de Química Inorgánica, Universidade de Vigo, Campus Universitario, E-36310, Vigo, Spain
[b] Dipartimento di Scienze Molecolari e Nanosistemi, Università Ca' Foscari Venezia, Via Torino 155, 30172, Mestre Venezia, Italy
[c] Departamento de Química Física, Universidade de Vigo, Campus Universitario, E-36310, Vigo, Spain

ARTICLE INFO

Article history:
Received 22 March 2018
Received in revised form
20 August 2018
Accepted 21 August 2018
Available online 23 August 2018

Keywords:
Ruthenium complexes
Trichlorostannyl ligand
Diphosphinite ligand
DFT
NBO

ABSTRACT

Trichlorostannyl complexes [Ru($SnCl_3$)(Cp')L] (**2a-c**) were prepared by treatment of optically active half-sandwich chlorocomplexes [RuCl(Cp')L] (**1a-c**) with an excess of $SnCl_2.2H_2O$ in ethanol. Treatment of trichlorostannyl complexes **2a-c** with $NaBH_4$ afforded trihydridostannyl derivatives [Ru(SnH_3)(Cp')L] (**3a-c**) in moderated yields. Treatment of **2a-c** with MgBrMe gave the trimethylstannyl complexes Ru($SnMe_3$)(Cp')L (**4a-c**). Alkynylstannyl derivatives [Ru{Sn(C≡CPh)$_3$}(Cp')L] (**5a-c**) were prepared by treatment of trichlorostannyl compounds **2a-c** with an excess of LiC≡CPh in thf. All the complexes present optical activity. The complexes were characterized spectroscopically and by X-ray crystal structure determination of [RuCl(η^5-C_5Me_5)L] (**1b**), [Ru($SnCl_3$)(η^5-C_5Me_5)L] (**2b**), and [Ru($SnCl_3$)(η^5-C_9H_7)L] (**2c**). The influence of different ligands on the Ru–P interaction in several complexes **1a-c**, **2a-c** and **3a-c** was evaluated by DFT calculations. These calculations indicate that $[SnCl_3]^-$ has a stronger stabilization effect than $[Cl]^-$ and the same occurs between $-C_9H_7$ and $-C_5Me_5$. These relative stabilities combined with the distortion energies of the fragments produce a stabilizing effect in the Ru–P bonds of complex **2c** that is twice as strong as in the **1b** complex.

1. Introduction

Although transition-metal complexes containing stannyl ligands have been known for a long time [1], a renewed interest has been growing in the recent decades [2] even extending to the actinides [3]. It is known that the introduction of a stannyl ligand may improve the catalytic properties of metal complexes [4]. Compounds containing trihalogen (SnX_3) offer the possibility of substituting the halogen (X) by H, OH, alkyl, …thus allowing us to obtain new ligands that can further modify the properties of the complexes. When the transition metal complexes display optical activity, their potential use in enantioselective catalysis poses an added value to the study of these compounds. Here we report the results of the studies on the synthesis, characterization and reactivity of chiral chloro-, and trichlorostannyl complexes of ruthenium stabilized by the half-sandwich fragments η^5-C_5H_5, η^5-C_5Me_5, and η^5-C_9H_7. In addition, the reactivity of the trichlorostannyl compounds with $NaBH_4$, methylmagnesium bromide and lithium phenylacetylide is also reported. The chiral environment was achieved using the auxiliary chiral diphosphinite ligand 1,2-[bis(diphenyl)phosphanyloxy]-1,2-diphenylethane (L) to complete the coordination sphere around the ruthenium atom. Metal complexes bearing chiral diphosphinite ligands have proved to be active in asymmetric catalysis [5]. Vicinal diphosphinites deserve special attention because of the similarities of their coordination to a metal center with the efficient DIOP ligand [6] We also report computational studies of the [RuX(Cp')L] X = Cl, $SnCl_3$, SnH_3; Cp' = η^5-C_5H_5, η^5-C_5Me_5, η^5-C_9H_7.

2. Results and discussion

The reaction diphenylchlorophosphine with enantiomerically pure diol (R,R)-(+)-hydrobenzoine in the presence of ^{n}BuLi, following procedure reported in the literature [7], led to formation of the optically active chelating ligand (R,R)-(+)-1,2-[bis(diphenyl)phosphanyloxy]-1,2-diphenylethane (**L**) as a white solid. The compound can be stored under Ar at room temperature for four

* Corresponding author.
E-mail address: sgarcia@uvigo.es (S. García-Fontán).

https://doi.org/10.1016/j.jorganchem.2018.08.017
0022-328X/

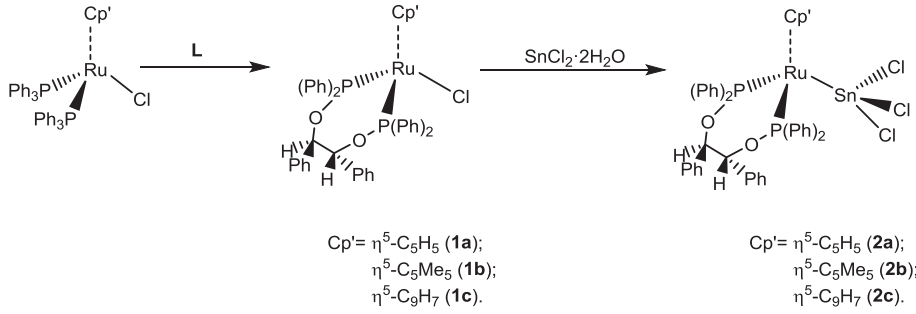

Scheme 1. Synthesis of the complexes [RuCl(Cp')L] (**1**) and [Ru($SnCl_3$) (Cp')L] (**2**).

weeks. After that its ^{31}P NMR spectrum shows small signals at $\delta \approx 20-40$ ppm corresponding to oxidation products.

The ^{1}H NMR spectrum in $CDCl_3$ shows multiplets at 6.85–7.80 ppm, corresponding to the phenyl groups and a multiplet at 5.08 ppm corresponding to the methylenic protons. The $^{31}P\{^{1}H\}$ NMR spectrum shows a singlet at 109.7 ppm, indicating the magnetic equivalence of the two phosphorus nuclei of diphosphinite ligand.

Synthesis and characterization of the half-sandwich chloro- and trichlorostannylcomplexes [RuCl(Cp')L] (1) and [Ru($SnCl_3$) (Cp')L] (2) Cp' = η^5-C_5H_5 (a), η^5-C_5Me_5 (b), η^5-C_9H_7 (c).

Optically active half-sandwich chlorocomplexes [RuCl(Cp')L] Cp' = η^5-C_5H_5 (**1a**), η^5-C_5Me_5 (**1b**), η^5-C_9H_7 (**1c**), were prepared by thermal displacement of PPh_3 from [(RuCl(Cp') (PPh_3)$_2$] complex by **L** in refluxing toluene, as shown in Scheme 1.

The new compounds are yellow **1a-b** or red-orange **1c** solids that are air-stable at room temperature and soluble in common organic solvents. Analytical and NMR spectroscopic data of compounds **1a-c** support the proposed formulation. Thus, the phosphorus nuclei of the bidentate ligand **L** are inequivalent and hence a two-doublet pattern corresponding to an AB spin system is observed in the $^{31}P\{^{1}H\}$ NMR spectra. The ^{1}H NMR spectra display, in addition to the characteristic signals of the carbocyclic ligands, a collapsed doublet of doublets and a doublets of doublets corresponding to the diastereotopic methylene protons of L (see Experimental).

Insertion of $SnCl_2$ into the Ru–Cl bond of complexes **1a-c** gave the trichlorostannyl complexes [Ru($SnCl_3$) (Cp')L] (**2a-c**) in moderate yields (50–58%) (Scheme 1). The new stannyl complexes were isolated as air and moisture stable crystalline yellow (**2a,b**) or orange (**2c**) solids. Analytical and NMR spectroscopy data support this formulation. Therefore, the ^{31}P NMR spectra of **2a-c** derivatives show two doublets (an AB system signal in the case of compound **2a**) with the characteristic satellites, due to coupling with the ^{119}Sn and ^{117}Sn nuclei of $SnCl_3$ ligand (Table 1). The ^{119}Sn NMR spectra also display a doublet of doublets (at −36.7 ppm for **2c**) or broad triplets (arising from the collapsed doublet of doublets with very similar coupling constants) at −7.4 ppm for **2a** and at −20.3 ppm for **2b**. The comparison of the ^{31}P NMR data of compounds **1** and **2** shows that the insertion of $SnCl_2$ has little or no influence on one of the P nuclei but produces a low field displacement on the other. This dissimilar behavior has already been reported for other complexes. So, in the case of [Ru(C_5H_5)Cl (dippe)] and [Ru(C_5Me_5)Cl (dippe)] the insertion of $SnCl_2$ does not affect the ^{31}P chemical shift [8c]; however for [Ru(C_5H_5)Cl (prophos)] [8f] and for [Ru(C_5H_5)Cl(PPh_3)$_2$] [8g] high and low field displacements were respectively observed. As expected, compounds **2a-c** present optical activity (see Experimental).

2.1. X-ray structures of 1 b, 2 b and 2c

The structure of compounds **1b, 2b** and **2c** was determined by X-ray diffraction studies. ORTEP drawings of these structures (Figs. 1–3) and selected bond lengths and angles (Table 2) are shown. The ruthenium atom is in a formally six-coordinate environment coordinated by the corresponding carbocyclic ligand, two

Table 1
$^{31}P\{^{1}H\}$ and $^{119}Sn\{^{1}H\}$ NMR data for compounds **1** and **2**.

	$^{31}P\{^{1}H\}$ NMR	$^{119}Sn\{^{1}H\}$ NMR
Comp	(δ/ppm; J/Hz)	(δ/ppm; J/Hz)
1a	δ_A 158.5, δ_B 153.1, $^{2}J_{AB} = 77.1$	
1b	δ_A 160.4, δ_B 156.6, $^{2}J_{AB} = 73.8$	
1c	δ_A 160.5, δ_B 157.5, $^{2}J_{AB} = 72.0$	
2a	δ_A 159.7 $^{2}J^{31}{}_{P}-^{119}{}_{Sn} \approx 468$, $^{2}J^{31}{}_{P}-^{117}{}_{Sn} \approx 448$ δ_B 158.7 $^{2}J^{31}{}_{P}-^{119}{}_{Sn} \approx 444$, $^{2}J^{31}{}_{P}-^{117}{}_{Sn} \approx 423$ $^{2}J_{AB} = 54.5$	−7.4 cdd[a], $^{2}J^{119}{}_{Sn}-^{31}{}_{P} \approx 458$
2b	170.5 d $^{2}J^{31}{}_{P}-^{119}{}_{Sn} \approx 427$, $^{2}J^{31}{}_{P}-^{117}{}_{Sn} \approx 406$ 156.5 d $^{2}J^{31}{}_{P}-^{119}{}_{Sn} \approx 422$, $^{2}J^{31}{}_{P}-^{117}{}_{Sn} \approx 403$ $^{2}J_{PP} = 55.1$	−20.3 cdd[a], $^{2}J^{119}{}_{Sn}-^{31}{}_{P} \approx 421$
2c	163.6 d $^{2}J^{31}{}_{P}-^{119}{}_{Sn} = 428.0$, $^{2}J^{31}{}_{P}-^{117}{}_{Sn} = 416.3$, 159.1 d $^{2}J^{31}{}_{P}-^{119}{}_{Sn} = 363.1$, $^{2}J^{31}{}_{P}-^{117}{}_{Sn} = 349.1$ $^{2}J_{PP} = 50.8$	−36.7 dd, $^{2}J^{119}{}_{Sn}-^{31}{}_{P} = 430.8$, $^{2}J^{119}{}_{Sn}-^{31}{}_{P} = 365.2$

In CD_2Cl_2 at 25 °C. [a] collapsed doublet of doublets.

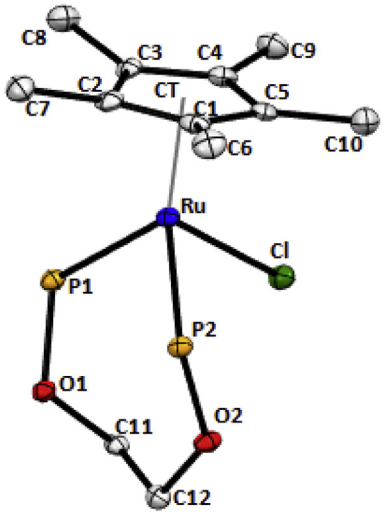

Fig. 1. ORTEP view (50% probability level) of compound **1b**. Hydrogen atoms and the phenyl groups are omitted for clarity.

phosphorous atoms from the bidentate ligand and a chloro (**1b**), or a trichlorostannyl (**2b, 2c)** groups. All molecules have a "three-legged piano stool" geometry with values near 90° for P (1)–Ru–P (2), P (1)–Ru–Sn and P (2)–Ru–Sn bond angles for compounds **2b** and **2c** and for P (1)–Ru–P (2), P (1)–Ru–Cl and P (2)–Ru–Cl for **1b**. The centroids of the carbocyclic ligands are situated at 1.884 (4) (**1b**) 1.905 (4) (**2b**) and 1.921 (2) Å (**2c**) from the ruthenium atom and the Ru–C, Ru–P, Ru–Cl and Ru–Sn bond lengths are similar to those observed for analog complexes [8]. It is worth mentioning that, in the case of compounds **1b** and **2b** both distances Ru–P (1) (2.242 Å (**1b**), 2.299 Å (**2b**)) and Ru–P (2) (2.255 Å (**1b**), 2.283 Å (**2b**)) are almost identical, but for compound **2c** they are significantly different (Ru–P (1) 2.283 Å, Ru–P (2) 2.237 Å), probably due to steric effects attributed to the asymmetry of the indenyl ligand. In fact the non-bonding distance between the center of the six-member ring of the indenyl group and P (1) (4.243 Å) is significantly shorter than for P (2) (5.302 Å) implying a stronger steric interaction of this group with the phenyl groups attached to the P (1) than with those attached to the P (2). The geometry around the center of Sn (II) is pyramidal trigonal with an average value for Sn–Cl bond distance of 2.3963 Å (**2b**) and 2.4045 Å (**2c**) and an average Cl–Sn–Cl angle of 92.61° (**2b**) and 95.38° (**2c**). These values are similar to those found in the analogous compounds in the literature [2 b,8 g].

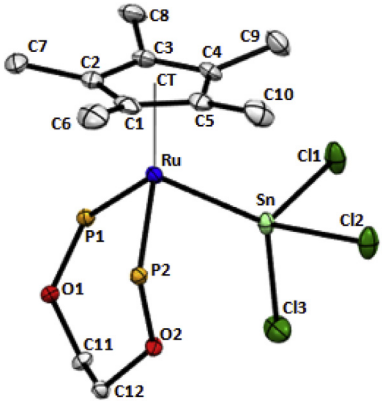

Fig. 2. ORTEP view (50% probability level) of compounds **2b.** Hydrogen atoms and the phenyl groups are omitted for clarity.

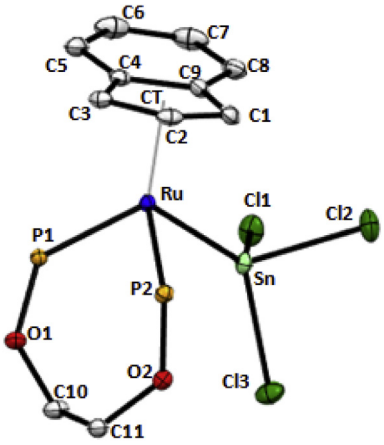

Fig. 3. ORTEP view (50% probability level) of compounds **2c.** Hydrogen atoms and the phenyl groups are omitted for clarity.

2.2. Reactivity of trichlorostannylcomplexes 2a-c

Treatment of compounds [Ru($SnCl_3$) (Cp')L] **2a-c** with $NaBH_4$ in ethanol at room temperature permits substitution of the three chlorides in the $SnCl_3$ group with H^-, affording the trihydridostannyl derivatives [Ru(SnH_3) (Cp')L] [Cp' = η^5-C_5H_5 (**3a**), η^5-C_5Me_5 (**3b**), η^5-C_9H_7 (**3c**)] in moderate yields (52–66%). It is worthy to mention that these compounds, together with those published by the Albertin group, are the only transition metal trihydridostannyl complexes published to date [2 b,c,e,f]. The compounds are yellow, stable in air for a few days and unstable in solutions of halogenated solvents. The IR spectra show a medium intensity band at about 1700 cm^{-1} attributed to the ν_{Sn-H} of the trihydridostannyl ligand [2d]. The ^1H NMR spectra confirm the presence of the SnH_3 ligand, showing a singlet at 4.28 ppm (**3a**), 4.45 ppm (**3b**), and 4.09 ppm (**3c**), with the characteristic satellites due to coupling with ^{119}Sn and ^{117}Sn nuclei. The values of these coupling constants are similar to those observed for similar complexes [2b,d]. The ^{31}P NMR spectra of compounds **3a-c** display signals corresponding to an AB spin system with the satellites due to coupling with the ^{119}Sn and ^{117}Sn nuclei of SnH_3 ligand. It was not possible to record the ^{119}Sn NMR spectra of compounds **3a-c** because of the aforementioned unstability of their solutions. Optical activity of these compounds is also observed.

Compounds [Ru($SnCl_3$) (Cp')L] **2a-c** react with nucleophiles like methylmagnesium bromide and lithium phenylacetylide to give new chiral triorganostannyl derivatives (Scheme 2). The reactions proceeded with the substitution of all the chlorides in $SnCl_3$. Thus, reaction of **2a-c** with an excess of MeMgBr in diethyl ether at room temperature gave the trimethylstannyl compounds [Ru($SnMe_3$) (Cp')L], [Cp' = η^5-C_5H_5 (**4a**), η^5-C_5Me_5 (**4b**), η^5-C_9H_7 (**4c**)] in moderate yields (52–65%). On the other hand, treatment of compounds **2a-c** with an excess of LiC≡CPh gave the tris(phenylacetylenide) stannyl compounds [Ru{Sn(C≡CPh)$_3$}(Cp')L], [Cp' = η^5-C_5H_5 (**5a**), η^5-C_5Me_5 (**5b**), η^5-C_9H_7 (**5c**)] in moderate yields (60–70%). Compounds **4a-c** and **5a-c** were obtained as air-stable yellow solids and their formulation was supported by analytical and spectroscopic (IR and NMR) data. The ^1H NMR spectra of compounds **4a-c** display, in addition to the expected signals for the diphosphinite and carbocyclic ligands, a singlet at 0.63 ppm (**4a**), 0.30 ppm (**4b**), and −0.09 ppm (**4c**), with the characteristic ^{119}Sn and ^{117}Sn satellites, integrating by nine protons, which can be attributed to the methyl groups bonded to Sn atom. The $^{13}C\{^1H\}$ NMR spectra show a singlet at −1.4 ppm ($J^{13}_C-^{119}_{Sn} = 80.6$ Hz) (**4a**), 1.4 ppm ($J^{13}_C-^{119}_{Sn} = 37.2$ Hz) (**4b**), and −2.0 ppm ($J^{13}_C-^{119}_{Sn} = 91.1$ Hz) (**4c**),

Table 2
Selected bond lengths (Å) and angles (°) for **1b**, **2b** and **2c**.

1b		2b		2c	
Ru–P (1)	2.242 (3)	Ru–P (1)	2.2990 (11)	Ru–P (1)	2.2830 (7)
Ru–P (2)	2.255 (3)	Ru–P (2)	2.2835 (10)	Ru–P (2)	2.2378 (7)
Ru–C (1)	2.219 (4)	Ru–C (1)	2.271 (4)	Ru–C (1)	2.240 (3)
Ru–C (2)	2.277 (4)	Ru–C (2)	2.269 (4)	Ru–C (2)	2.215 (3)
Ru–C (3)	2.266 (4)	Ru–C (3)	2.255 (4)	Ru–C (3)	2.206 (3)
Ru–C (4)	2.235 (4)	Ru–C (4)	2.265 (4)	Ru–C (4)	2.349 (3)
Ru–C (5)	2.239 (4)	Ru–C (5)	2.254 (4)	Ru–C (9)	2.350 (3)
Ru-CT	1.884 (4)	Ru-CT	1.905 (4)	Ru-CT	1.921 (2)
Ru–Cl	2.433 (3)	Ru–Sn	2.5655 (4)	Ru–Sn	2.5871 (3)
		Sn–Cl (1)	2.3991 (11)	Sn–Cl (1)	2.4041 (7)
		Sn–Cl (2)	2.3936 (11)	Sn–Cl (2)	2.4003 (7)
		Sn–Cl (3)	2.3963 (12)	Sn–Cl (3)	2.4091 (7)
CT-Ru–P (1)	129.68 (6)	CT-Ru–P (1)	128.4 (2)	CT′–Ru–P (1)	127.22 (2)
CT-Ru–P (2)	128.95 (6)	CT-Ru–P (2)	125.57 (15)	CT′–Ru–P (2)	123.65 (2)
P (1)–Ru–P (2)	88.75 (7)	P (1)–Ru–P (2)	90.04 (4)	P (1)–Ru–P (2)	90.93 (2)
CT-Ru–Cl	116.87 (14)	CT-Ru–Sn	119.22 (10)	CT′–Ru–Sn	114.818 (10)
P (1)–Ru–Cl	92.67 (7)	P (1)–Ru–Sn	92.84 (3)	P (1)–Ru–Sn	100.73 (2)
P (2)–Ru–Cl	88.24 (5)	P (2)–Ru–Sn	90.49 (3)	P (2)–Ru–Sn	91.83 (2)
		Cl (3)–Sn–Cl (1)	95.08 (5)	Cl (3)–Sn–Cl (1)	97.57 (3)
		Cl (3)–Sn–Cl (2)	93.32 (4)	Cl (3)–Sn–Cl (2)	92.50 (3)
		Cl (2)–Sn–Cl (1)	89.44 (4)	Cl (2)–Sn–Cl (1)	96.07 (3)

CT: centroid at Cp*; CT': centroid at the five-member ring of C_9H_7.

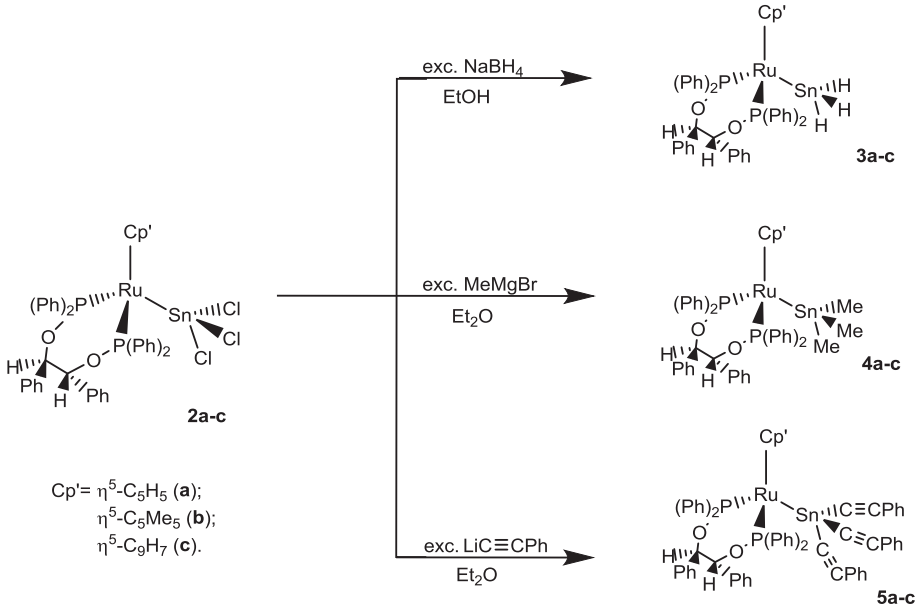

Scheme 2. Synthesis of the complexes [Ru(SnH_3) (Cp')L] (**3**); [Ru($SnMe_3$) (Cp')L] (**4**); [Ru{Sn(C≡CPh)$_3$}(Cp')L] (**5**).

correlating, in a HSQC experiment, with the corresponding, above-mentioned, proton singlet. The proton-coupled ^{119}Sn NMR spectrum of compound **4c** shows a triplet of multiplets arising from the coupling with the two P nuclei of the bidentate ligand and the nine protons of the three methyl groups.

The IR spectra of compounds **5** present a medium-intensity broad band at 2124 cm^{-1} (**5a**) 2127 cm^{-1} (**5b**) and 2125 cm^{-1} (**5c**) that can be attributed to the $\nu_{C\equiv C}$ of the Sn(C≡CPh)$_3$ group [8]. Besides, the presence of the acetylide group bonded to the tin atom can be confirmed by the $^{13}C\{^1H\}$ and $^{119}Sn\{^1H\}$ NMR spectra. Thus, the $^{13}C\{^1H\}$ NMR spectra display, in addition to the characteristic signals of the supporting ligands, two singlets [$\delta = 107.5$ and $\delta = 100.7$ ppm (**5a**), $\delta = 107.2$ and $\delta = 103.3$ ppm (**5b**), and $\delta = 107.2$ and $\delta = 99.6$ (**5c**)], attributed to C_β and C_α, respectively, of the Sn(C_α≡C_βPh)$_3$ group. The $^{119}Sn\{^1H\}$ NMR spectra shows a collapsed doublet of doublets at $\delta = -248.5$ ppm (**5a**) and a doublet of doublets at $\delta = -233.2$ ppm (**5b**) and at $\delta = -267.0$ ppm (**5c**), due to the coupling of the tin nucleus with the two non-equivalent P atoms of the chiral ligand.

^{31}P NMR data for compounds **3**–**5** are very similar suggesting that the modification of the groups attached to the Sn atom has little influence on the P atoms of the diphosphinite ligand.

Bimetallic compounds Ru-SnR_3 (R = H, Me, C≡CPh) **3**–**5** are the first to contain a chiral phosphinite bidentate ligand.

2.3. Computational studies

Full optimizations at B3LYP/cc-pVDZ (–PP) [9] level of theory were performed in ground state for complexes **1a-c**, **2a-c** and **3a-c**, for the phosphinite ligand (**L**) and for the moieties resulting from removing the phosphinite from the different complexes. Frequency and force constants were obtained at the same level of theory and

the minimum nature of each geometry was established. Next, a natural bond orbital (NBO) analysis [10] was done together with obtaining the Wiberg bond indices (WBI) [11] and performing a natural population analysis (NPA) [12]. The most relevant distances of the studied compounds are listed in Table 3 along with the NPA charges, Wiberg bond indices, NBO populations and NBO energies.

The distances in Table 3 show that the η^5-C_9H_7 moiety breaks to a certain extent the equivalence of the two Ru–P bonds in complexes **1c**, **2c** and **3c**. This is confirmed by the Wiberg bond indices and the values of the NPA charges. In complexes with the η^5-C_5Me_5 or the η^5-C_5H_5 moiety the differences between the two phosphorus atoms are very small, suggesting a similar strength and nature of the two Ru–P interactions of each compound. The obtained value of the Wiberg bond indices for the Ru–P bonds goes from 0.79 to 0.90, which points to a covalent nature of these bonds in all cases. The calculated NPA charges reveal that the Ru–P bonds are highly polarized for all complexes, with charges from 1.53 a. u. to 1.64 a. u. on the phosphorus atoms and from −0.73 a. u to −1.30 a. u on the ruthenium atom. The substitution of chloride by the $SnCl_3$ or the SnH_3 moieties increases the charge on the ruthenium atom in about −0.4 a. u, which leads to a further polarization of the Ru–P bonds. NBO isosurfaces displayed in the Supporting Information do not show significant differences in size or shape between the complexes. As can be seen in Table 3, the occupancy of all compounds is rather alike, but the combined effect of the chloride or of the SnH_3 and η^5-C_9H_7 ligands breaks the equivalence of Ru–P bonds in complexes **1c** and **3c**. These compounds have, in general, the bigger differences between Ru–P bonds for all studied properties, i. e WBI, NPA charges, NBO populations and NBO energies. It is not clear if the asymmetry plays any role in it, but complex **1c** has also the most stable Ru–P bonds according to the NBO energies.

By analyzing the distortion and the interaction energies in the complexes, we can perform an estimation of how the ligands modify the Ru–P interactions. In order to carry out this analysis a fragment-based approach is used in which a decomposition of the total energy of the complex (ΔE_{tot}) is performed. This energy is divided in two terms, i.e. the interaction energy between two fragments (ΔE_{int}) and the energy associated with distorting these fragments from their initial equilibrium structures (ΔE_{dist}). Thus, $\Delta E_{tot} = \Delta E_{int} + \Delta E_{dist}$. The calculated results are given in Table 4 together with the Basis Set Superposition Error (BSSE) [13]. The fragments selected for our study were, on the one hand, the phosphinite ligand (**L**) and on the other, the remaining [RuCl(Cp')], [Ru($SnCl_3$) (Cp')] and [Ru(SnH_3) (Cp')] for the complexes **1a-c**, **2a-c** and **3a-c**, respectively. A further explanation of how those energies have been obtained is given in the Supporting Information.

The values of the interaction energy are very stabilizing, with energies of one Ru–P interaction from about −40 kcal/mol up to approximately −55 kcal/mol, considering that both Ru–P bonds of the same complex have roughly the same energy. Like in the NBO analysis, the compound [RuCl(η^5-C_5Me_5)L] (**1b**) has the less stable interactions. Yet, in contrast with NBO results the complex with the most stable interactions is the [Ru($SnCl_3$) (η^5-C_9H_7)L] (**2c**). Differences in the BSSE values are not enough to produce any significant change in the relative stabilities between complexes. The values of ΔE_{dist} are large, which reduces notably the stabilization of the complexes with respect to the interaction energies. The energy required for the geometrical distortion of **L** is rather similar for all complexes but large differences are found when the distortion energy of the [RuCl(Cp')] or [Ru($SnCl_3$) (Cp')] fragment is considered. Thus, this energy for [RuCl(η^5-C_5Me_5)L] (**1b**) and [RuCl(η^5-C_9H_7)L] (**1c**) is almost three times as big as that for [Ru($SnCl_3$) (η^5-C_5H_5)L] (**2a**), which produces a much larger destabilization of the two former complexes. In [RuCl(η^5-C_5Me_5)L] (**1b**), the large distortion energy of the [RuCl(η^5-C_5Me_5)] moiety is mainly due to the distortion of the Ru–Cl bond. In the equilibrium geometry of the fragment, this bond is collinear with the axis defined by the apothem of the η^5-C_5Me_5 and the ruthenium atom, but in the complex **1b** it is placed forming an angle of around 61° with this axis. This effect, combined with a rotation of the Ru–Cl bond around the symmetry axis, is responsible for the large distortion energy in [RuCl(η^5-C_9H_7)L] (**1c**).

When a comparison of the total energies is performed, we can establish the following correlation of ligands regarding the stability of the Ru–P interactions, from less stable Ru–P bonds to more stable bonds: η^5-$C_5Me_5 < \eta^5$-$C_5H_5 \approx \eta^5$-C_9H_7 and $[Cl]^- \ll [SnH_3]^- < [SnCl_3]^-$. Thus, the relatively low stabilization of the Ru–P interactions in the complex [RuCl(η^5-C_5Me_5)L] (**1b**) is the combination of several effects: a1) the lower stabilization effect of the η^5-C_5Me_5 with respect to η^5-C_9H_7 and η^5-C_5H_5; a2) the lower stabilization effect of the chloride ligand with respect to the stannyl ligands; b1) the lower distortion energy of η^5-C_9H_7 and η^5-C_5H_5 regarding η^5-C_5Me_5; b2) the lower distortion energy of the stannyl ligands regarding the chloride ligand. The energy results suggest that less polarized Ru–P bonds together with large distortions will

Table 4
B3LYP/cc-pVDZ (−PP) distortion (ΔE_{dist}), BSSE, interaction (ΔE_{int}) and total (ΔE_{tot}) energies (kcal/mol) computed for compounds **1**–**3**.

	ΔE_{int}	BSSE	ΔE_{dist} (L)	ΔE_{dist} [Ru(X) (Cp')]*	ΔE_{dist} (total)	ΔE_{tot}
1a	−90.21	6.36	12.38	23.13	35.51	−54.70
1b	−83.50	7.40	12.86	28.71	41.57	−41.93
1c	−98.20	6.83	13.08	27.19	40.27	−57.93
2a	−105.81	7.80	11.88	9.69	21.57	−84.23
2b	−94.35	8.82	13.82	17.04	30.86	−63.49
2c	−109.10	8.26	12.80	12.52	25.32	−83.78
3a	−99.61	5.78	10.95	10.21	21.16	−78.45
3b	−92.79	6.95	13.35	16.62	29.97	−62.81
3c	−103.95	6.11	11.39	12.22	23.61	−80.34

[Ru(X) (Cp')]*X = Cl; $SnCl_3$; SnH_3.

Table 3
Selected bond lengths (Angstroms), Wiberg bond indices, NPA atomic charges (atomic units) and NBO energies (eV) and populations (atomic units) for compounds **1**–**3**.

	1a	1 b	1c	2a	2 b	2c	3a	3 b	3c
$\mathbf{r}_{Ru\text{-}P1}$	2.300	2.323	2.269	2.326	2.363	2.299	2.286	2.310	2.267
$\mathbf{r}_{Ru\text{-}P2}$	2.309	2.341	2.314	2.329	2.372	2.343	2.288	2.313	2.300
$\mathbf{WBI}_{Ru-P1}$	0.86	0.82	0.89	0.84	0.79	0.86	0.89	0.85	0.90
$\mathbf{WBI}_{Ru-P2}$	0.85	0.81	0.82	0.84	0.79	0.80	0.88	0.85	0.84
$\mathbf{q}_{Ru}$	−0.84	−0.73	−0.74	−1.30	−1.16	−1.15	−1.27	−1.14	−1.11
$\mathbf{q}_{P1}$	1.60	1.55	1.64	1.59	1.54	1.62	1.60	1.55	1.62
$\mathbf{q}_{P2}$	1.61	1.56	1.56	1.60	1.53	1.55	1.60	1.55	1.56
$\mathbf{E}_{Ru\text{-}P1}$	−12.72	−12.06	−13.52	−13.05	−12.70	−12.21	−12.13	−12.78	−12.00
$\mathbf{E}_{Ru\text{-}P2}$	−12.36	−12.40	−13.00	−12.86	−12.77	−12.33	−12.92	−12.55	−13.03
$\mathbf{Pop}_{Ru\text{-}P1}$	1.92	1.89	1.93	1.92	1.92	1.90	1.85	1.92	1.90
$\mathbf{Pop}_{Ru\text{-}P2}$	1.92	1.92	1.84	1.92	1.92	1.88	1.82	1.92	1.84

produce lower stabilizations. As has also been pointed out above, the inclusion of the BSSE in the total energies will not change the outcome of the discussion.

3. Conclusions

In this work, we reported that cyclopentadienyl, pentamethylcyclopentadienyl and indenyl ligands in fragment [RuCp'L] (L = phosphinite) can stabilize trichlorostannyl ([Ru]–$SnCl_3$), trihydridostannyl ([Ru]–SnH_3) and organostannyl derivatives ([Ru]-$SnMe_3$) and ([Ru]-Sn(C≡CPh)$_3$).

The calculated NPA charges reveal highly polarized Ru–P bonds. The substitution of the chlorine by a $[SnCl_3]^-$ or a $[SnH_3]^-$ moiety increases the negative charge on the ruthenium atom. The influence of the ligands on the Ru–P interactions was further evaluated by means of a distortion/interaction analysis. The ΔE_{int} values show that the stabilization trends are η^5-$C_5Me_5 < \eta^5$-$C_5H_5 \approx \eta^5$-C_9H_7 and $[Cl]^- \ll [SnH_3]^- < [SnCl_3]^-$.

4. Experimental section

4.1. General considerations

All experiments were carried out under an atmosphere of argon by Schlenk techniques. Solvents were dried by the usual procedures [14] and, prior use, distilled under argon. The starting materials [RuCl(η^5-C_5H_5) (PPh_3)$_2$] [15], [RuCl(η^5-C_5Me_5) (PPh_3)$_2$] [16] and [RuCl(η^5-C_9H_7) (PPh_3)$_3$] [17] were prepared as described in the literature. All reagents were obtained from commercial sources. NMR spectra were recorded at room temperature on Bruker ARX-400, Bruker DPX-600 instrument, with resonating frequencies 400 MHz (^{1}H), 161 MHz (^{31}P{^{1}H}), 100 MHz (^{13}C{^{1}H}), and 223 MHz (^{119}Sn and ^{119}Sn{^{1}H}) using the solvents as the internal lock. ^{1}H and ^{13}C{^{1}H} signals are referred to internal TMS, those of ^{31}P{^{1}H} to 85% H_3PO_4 and ^{119}Sn shifts with respect to Sn(CH_3)$_4$; downfield shifts (expressed in ppm) are considered positive. ^{1}H and ^{13}C{^{1}H} NMR signal assignments were confirmed by {^{1}H, ^{1}H} COSY, {^{1}H, ^{13}C} HSQC and DEPT experiments. Coupling constants are given in hertz. Infrared spectra were run on a Jasco FT/IR (ATR) spectrometer. C, H analyses were carried out with a Carlo Erba 1108 analyzer. Optical rotation values were recorded on a Jasco P-2000 polarimeter.

4.2. Preparation of $Ph_2POCHPhCHPhOPPh_2$ (**L**).[7]

A round-bottom flask was charged with a mixture of (R,R)-(+)-hydrobenzoin (1.00 g, 4.71 mmol) and 10 mL of THF. The solution was cooled to 0 °C and 3.8 mL of ^{n}BuLi (9.42 mmol, 2.5 M solution in hexane) were added dropwise. Then, 1.8 mL of Ph_2PCl (9.42 mmol) were slowly added. The reaction mixture was allowed to reach room temperature, filtered with a cannula, and the filtrate was concentrated under reduced pressure to produce a white oil. The oil obtained was stirred with ethanol (20 mL) resulting in a white solid which was filtered, washed with ethanol (10 mL) and dried under reduced pressure.

Yield: 56%. Anal. Calc for $C_{38}H_{32}O_2P_2$ (582.62): C, 78.34; H, 5.54. Found: C, 78.68; H, 5.23.^{1}H NMR ($CHCl_3$-d_1, 25 °C) δ: 7.80–6.85 (m, 30H, Ph), 5.08 (m, 2H, C<u>H</u> L) ppm. ^{31}P{^{1}H} NMR ($CHCl_3$-d_1, 25 °C) δ: 109.7 (s) ppm. $[\alpha]_D^{27}$: 25.7 (*c* 0.06, $CHCl_3$).

4.3. Synthesis of complexes

4.3.1. [RuCl(Cp')L] [Cp' = η^5-C_5H_5 (**1a**), η^5-C_5Me_5 (**1b**), η^5-C_9H_7 (**1c**)]

An excess of $Ph_2POCHPhCHPhOPPh_2$ (**L**) (0.70 mmol) was added to a solution of [(RuCl(Cp') (PPh_3)$_2$] (0.64 mmol) in toluene (30–40 mL). The reaction mixture was refluxed for 3 h and allowed to cool to room temperature. The solvent was removed under vacuum, and the residue was treated with ethanol (3 mL), affording products that yellow (**1a**, **1b**) or red-orange (**1c**) that were filtered and crystallized from CH_2Cl_2 and ethanol (2:5).

(1a) Yield: 79%. Anal. Calc. for $C_{43}H_{37}ClO_2P_2Ru$ (784.24): C, 65.86; H, 4.76. Found: C, 65.92; H, 4.65.^{1}H NMR (CH_2Cl_2-d_2 (25 °C) δ: 7.70–6.70 (m, 30H, Ph), 6.03 (dd, $^3J_{H-H}$ = 7.6 Hz, $^3J_{H-P}$ = 14.2 Hz, 1H, C<u>H</u> L), 5.16 (cdd, $^3J_{H-H}$ = 7.6 Hz, 1H, C<u>H</u> L), 4.51 (s, 5H, C_5<u>H_5</u>) ppm. ^{31}P{^{1}H} NMR (CH_2Cl_2-d_2, 25 °C) δ: AB system, δ_A 158.5, δ_B 153.1 ($^2J_{AB}$ = 77.1 Hz) ppm. $[\alpha]_D^{23}$: 120.2 (*c* 0.20, C_6H_6).

(1b) Yield: 70%. Anal. Calc. for $C_{48}H_{47}ClO_2P_2Ru$ (854.17): C, 67.43; H, 5.55. Found: C, 67.76; H, 5.42.^{1}H NMR (CH_2Cl_2-d_2, 25 °C) δ: 7.75–6.45 (m, 30H, Ph), 5.78 (dd, $^3J_{H-P}$ = 13.4 Hz, $^3J_{H-H}$ = 7.9 Hz, 1H, C<u>H</u> L), 4.98 (dd, $^3J_{H-H}$ = 7.9 Hz, $^3J_{H-P}$ = 2.8 Hz, 1H, C<u>H</u> L), 1.23 (s, 15H, C_5<u>Me_5</u>) ppm. ^{31}P{^{1}H} NMR (CH_2Cl_2-d_2, 25 °C) δ: AB system, δ_A 160.4, δ_B 156.6 ($^2J_{AB}$ = 73.8 Hz) ppm. $[\alpha]_D^{27}$: −40.3 (*c* 0.19, $CHCl_3$).

(1c) Yield: 78% Anal. Calc. for $C_{47}H_{39}ClO_2P_2Ru$ (834.30): C, 67.66; H, 4.71. Found: C, 67.32; H, 4.80.^{1}H NMR (400 MHz, CH_2Cl_2-d_2, 25 °C): δ 7.86–6.47 (m, 30H, Ph, C_9H_7), 5.91 (dd, $^3J_{H-P}$ = 13.1 Hz, $^3J_{H-H}$ = 8.2 Hz, C<u>H</u> L), 5.15 (m, 1H, C<u>H</u> L), 4.68 (m, 1H, H_2, C_9H_7), 4.21 (s, 1H, $H_{1,3}$, C_9H_7), 4.10 (s, 1H, $H_{1,3}$, C_9H_7). ^{31}P{^{1}H} NMR (161 MHz, CH_2Cl_2-d_2, 25 °C) δ: AB system, δ_A 160.5, δ_B 157.5 ($^2J_{AB}$ = 72 Hz). ^{13}C{^{1}H} NMR (CH_2Cl_2-d_2, 25 °C) δ: 146.9–127.4 (m, Ph + C_{5-8} C_9H_7), 117.5 (d, $^2J_{C-P}$ = 5.1 Hz, $C_{4,9}$ C_9H_7), 109.2 (d, $^2J_{C-P}$ = 7.3 Hz, $C_{4,9}$ C_9H_7), 89.3 (s, C_2 C_9H_7), 85.2 (dd, $^2J_{C-P}$ = 8.7 Hz, $^3J_{C-P}$ = 1.8 Hz, C<u>H</u> L), 80.8 (d, $^2J_{C-P}$ = 2.4 Hz, $C_{1,3}$ C_9H_7), 70.4 (d, $^2J_{C-P}$ = 14.2 Hz, C<u>H</u> L), 64.8 (s, $C_{1,3}$ C_9H_7) ppm. $[\alpha]_D^{27}$: −141.1 (*c* 0.08, $CHCl_3$).

4.3.2. Preparation of [Ru($SnCl_3$) (Cp')L] [Cp' = η^5-C_5H_5 (**2a**), η^5-C_5Me_5 (**2b**), η^5-C_9H_7 (**2c**)]

A Schlenk tube was charged with 0.25 mmol of [RuCl(Cp')L] (**1a-c**) and $SnCl_2.2H_2O$ (0.95 mmol) in 20 mL of ethanol. The reaction mixture was refluxed for 2 h and then the solvent was removed under reduce pressure to give a residue was treated with hexane (2 mL), affording products that yellow (**2a**, **2b**) or orange (**2c**) that were filtered and washed with hexane and dried under vacuum.

(2a) Yield: 58%. Anal. Calc. for $C_{43}H_{37}Cl_3O_2P_2RuSn$ (973.83): C, 53.04; H, 3.83. Found: C, 52.89; H, 3.92.^{1}H NMR (CH_2Cl_2-d_2, 25 °C): δ 7.78–6.85 (m, 30H, Ph), 5.93 (dd, $^3J_{H-H}$ = 8.0 Hz, $^3J_{H-P}$ = 11.6 Hz, 1H, C<u>H</u> L), 5.02 (cdd, $^3J_{H-H}$ = $^3J_{H-P}$ = 8.0 Hz, 1H, C<u>H</u> L), 4.87 (s, 5H, C_5<u>H_5</u>) ppm. ^{31}P{^{1}H} NMR (CH_2Cl_2-d_2, 25 °C): δ AB, δ_A 159.7 ($^2J_{P-^{119}Sn}$ ≈ 468 Hz, $^2J_{P-^{117}Sn}$ ≈ 448 Hz), δ_B 158.7 ($^2J_{P-^{119}Sn}$ ≈ 444 Hz, $^2J_{P-^{117}Sn}$ ≈ 423 Hz) ($^2J_{AB}$ = 54.5 Hz) ppm. ^{119}Sn{^{1}H} NMR (CH_2Cl_2-d_2, 25 °C): δ −7.4 (cdd, $^2J_{Sn-P}$ ≈ 458 Hz). $[\alpha]_D^{27}$: 125.6 (*c* 0.20, CH_2Cl_2).

(2b) Yield: 56%. Anal. Calc. for $C_{48}H_{47}Cl_3O_2P_2RuSn$ (1044.01): C, 55.17; H, 4.54. Found: C, 55.10; H, 4.55%. ^{1}H NMR (CH_2Cl_2-d_2, 25 °C): δ 7.82–6.70 (m, 30H, Ph), 5.94 (dd, $^3J_{H-P}$ = 11.8 Hz, $^3J_{H-H}$ = 7.8 Hz, 1H, C<u>H</u> L), 4.77 (dd, $^3J_{H-P}$ = 9.5 Hz, $^3J_{H-H}$ = 7.8 Hz, 1H, C<u>H</u> L), 1.41 (s, 15H, C_5<u>Me_5</u>) ppm. ^{31}P{^{1}H} NMR (CH_2Cl_2-d_2, 25 °C): δ 170.5 (d, $^2J_{PP}$ = 55.1 Hz, $^2J_{P-119Sn}$ ≈ 427 Hz, $^2J_{P-117Sn}$ ≈ 406 Hz), 156.5 (d, $^2J_{PP}$ = 55.1 Hz, $^2J_{P-119Sn}$ ≈ 422 Hz, $^2J_{P-117Sn}$ ≈ 403 Hz) ppm. ^{13}C{^{1}H} NMR (CH_2Cl_2-d_2, 25 °C): δ 144.3–127.3(Ph), 94.8 (s, <u>C</u>$_5$Me$_5$), 85.9 (d, $^2J_{C-P}$ = 8.7 Hz, <u>C</u>H L), 83.2 (d, $^2J_{C-P}$ = 6.6 Hz, <u>C</u>H L), 10.1 (s, C_5<u>Me_5</u>) ppm. ^{119}Sn{^{1}H} NMR (CH_2Cl_2-d_2, 25 °C): δ −20.3 (cdd, $^2J_{Sn-P}$ ≈ 421 Hz) ppm. $[\alpha]_D^{27}$: 27.3 (*c* 0.20, $CHCl_3$).

(2c) Yield: 50%. Anal. Calc. for $C_{47}H_{39}Cl_3O_2P_2RuSn$ (1023.95): C, 55.08; H, 3.84. Found: C, 55.06; H, 3.90%. ^{1}H NMR (CH_2Cl_2-d_2, 25 °C): δ 8.30–6.15 (34H, Ph + H_{5-7} C_9H_7), 5.68 (dd, $^3J_{H-P}$ = 12.1 Hz, $^3J_{H-H}$ = 8.1 Hz, 1H, C<u>H</u> L), 5.22 (br d, $^3J_{H-H}$ = 2.5 Hz, 1H, H_2 C_9H_7), 5.07 (br s, 1H, $H_{1,3}$ C_9H_7), 4.94 (dd, $^3J_{H-P}$ = 9.2 Hz, $^3J_{H-H}$ = 8.1 Hz, 1H, C<u>H</u> L), 4.59 (br s, 1H, $H_{1,3}$ C_9H_7) ppm. ^{13}C{^{1}H} NMR (CH_2Cl_2-d_2, 25 °C): δ 146.2–124.1 (Ph + C_{5-8} C_9H_7), 110.0 (d, $^2J_{C-P}$ = 2.7 Hz, $C_{4,9}$ C_9H_7), 104.2 (d, $^2J_{C-P}$ = 3.7 Hz, $C_{4,9}$ C_9H_7), 88.7 (br s, C_2 C_9H_7), 86.7 (dd, $^2J_{C-P}$ = 9.8 Hz, $^3J_{C-P}$ = 1.1 Hz, <u>C</u>H L), 82.7 (br d, $^2J_{C-P}$ = 5.7 Hz, <u>C</u>H L), 73.5

(s, $C_{1,3}$ C_9H_7), 69.2 (br d, $^2J_{C\text{-}P} = 6.5$ Hz, $C_{1,3}$ C_9H_7) ppm. $^{31}P\{^1H\}$ NMR (CH_2Cl_2-d_2, 25 °C) δ: 163.6 (d, $^2J_{PP} = 50.8$ Hz, $^2J_{P\text{–}^{119}Sn} = 428.0$ Hz, $^2J_{P\text{–}^{117}Sn} = 416.3$ Hz), 159.1 (d, $^2J_{PP} = 50.8$, $^2J_{P\text{–}^{119}Sn} = 363.1$ Hz, $^2J_{P\text{–}^{117}Sn} = 349.1$ Hz) ppm. $^{119}Sn\{^1H\}$ NMR (CH_2Cl_2-d_2, 25 °C): δ −36.7 (dd, $^2J_{Sn\text{-}P} = 430.8$ Hz, $^2J_{Sn\text{-}P} = 365.2$ Hz) ppm. $[\alpha]_D^{27}$: −170.6 (*c* 0.19, $CHCl_3$).

4.3.3. [Ru(SnH$_3$) (Cp')L][Cp' = η^5-C_5H_5 (**3a**), η^5-C_5Me_5 (**3b**), η^5-C_9H_7 (**3c**)]

An excess of $NaBH_4$ (1.00 mmol) in 20 mL of ethanol was added to a suspension of [Ru($SnCl_3$) (Cp')L] (**2a-c**) (0.05 mmol) in ethanol. The reaction mixture was stirred at room temperature for 1 h and then the solvent was removed under vacuum giving a yellow solid. The complex was extracted from this solid with 15 mL of toluene using a celite® column for filtration. Extracts were evaporated to dryness to give an orange oil that was treated with ethanol (3 mL) giving a yellow product that was filtered out and dried under vacuum.

(3a) Yield: 52%. Anal. Calc. for $C_{43}H_{40}O_2P_2RuSn$ (870.50): C, 59.33; H, 4.63. Found: C, 59.70; H, 5.01%. FT-IR (ATR): $\nu_{Sn\text{-}H}$ 1730 (m) cm^{-1} ^1H NMR (C_6H_6-d_6, 25 °C); δ 8.00–6.70 (m, 30H, Ph), 6.24 (dd, $^3J_{H\text{-}P} = 11.6$ Hz, $^3J_{H\text{-}H} = 8.4$ Hz, 1H, C<u>H</u> L), 5.32 (cdd, $^3J_{H\text{-}P} = {}^3J_{H\text{-}H} = 8.4$ Hz, 1H, C<u>H</u> L), 4.60 (br s, 5H, $C_5\underline{H}_5$), 4.28 (s, $J_{H\text{-}^{119}Sn} = 1262.1$ Hz, $J_{H\text{-}^{117}Sn} = 1206.1$ Hz, 3H, SnH_3) ppm. $^{31}P\{^1H\}$ NMR (C_6H_6-d_6, 25 °C) δ: AB system, δ_A 163.7, ($^2J_{P\text{-}119Sn} \approx 289$ Hz, $^2J_{P\text{-}117Sn} \approx 277$ Hz), δ_B 160.1 ($^2J_{P\text{-}119Sn} \approx 297$ Hz, $^2J_{P\text{-}117Sn} \approx 285$ Hz) ($^2J_{AB} = 62.0$ Hz) ppm. $^{119}Sn\{^1H\}$ NMR (C_6H_6-d_6, 25 °C) δ: ABMX$_3$ system $\delta_M = -323.2$ ppm $[\alpha]_D^{27}$: 144.8 (*c* 0.20, C_6H_6).

(3b) Yield: 57%. Anal. Calc. for $C_{48}H_{50}O_2P_2RuSn$ (942.13): C, 61.14; H, 5.35. Found: C, 61.62; H, 5.60%. FT-IR (ATR): $\nu_{Sn\text{-}H}$ 1698 (m) cm^{-1}.^1H NMR (C_6H_6-d_6, 25 °C): δ 8.12–6.45 (m, 30H, Ph), 6.08 (dd, $^3J_{H\text{-}P} = 12.4$ Hz, $^3J_{H\text{-}H} = 7.9$ Hz, 1H, C<u>H</u> L), 5.16 (dd, $^3J_{H\text{-}H} = 7.9$ Hz, $^3J_{H\text{-}P} = 6.4$ Hz, 1H, C<u>H</u> L), 4.45 (s, $J_{H\text{-}^{119}Sn} = 1204.0$ Hz, $J_{H\text{-}^{117}Sn} = 1152.1$ Hz, 3H, SnH_3), 1.43 (br s, 15H, $C_5\underline{Me}_5$) ppm. $^{31}P\{^1H\}$ NMR (C_6H_6-d_6, 25 °C) δ: AB system, δ_A 165.7, δ_B 163.8 ($^2J_{AB} = 60.2$ Hz) ppm. $[\alpha]_D^{27}$: −58.5 (*c* 0.20, Toluene).

(3c) Yield: 66%. Anal. Calc. for $C_{47}H_{42}O_2P_2RuSn$ (922.07): C, 61.17; H, 4.59. Found: C, 59.41; H, 4.45%. FT-IR (ATR): $\nu_{Sn\text{-}H}$ 1738 (m) cm^{-1}.^1H NMR (C_6H_6-d_6, 25 °C): δ 8.20–6.25 (m, 34H, Ph + $H_{5\text{-}7}$ C_9H_7), 5.85 (dd, $^3J_{H\text{-}P} = 12.2$ Hz, $^3J_{H\text{-}H} = 8.0$ Hz, 1H, C<u>H</u> L), 5.21 (t, $^3J_{H\text{-}H} = 2.6$ Hz, 1H, H_2 C_9H_7), 5.04 (cdd, $^3J_{H\text{-}P} = {}^3J_{H\text{-}H} = 7.2$ Hz, 1H, C<u>H</u> L), 4.70 (s, 1H, $H_{1,3}$ C_9H_7), 4.60 (s, 1H, $H_{1,3}$ C_9H_7), 4.09 (s, $J_{H\text{-}^{119}Sn} = 1316$ Hz, $J_{H\text{-}^{117}Sn} = 1256$ Hz, 3H, SnH_3) ppm. $^{31}P\{^1H\}$ NMR (C_6H_6-d_6, 25 °C) δ: AB system, δ_A 165.3 ($^2J_{P\text{-}^{119}Sn} \approx 266.0$ Hz, $^2J_{P\text{-}^{117}Sn} \approx 256.0$ Hz), δ_B 163.8 ($^2J_{P\text{-}^{119}Sn} \approx 288.0$ Hz, $^2J_{P\text{-}^{117}Sn} \approx 276.0$ Hz) ($^2J_{AB} = 55.9$ Hz) ppm. $[\alpha]_D^{27}$: −123.3 (c 0.20, C_6H_6).

4.3.4. [Ru(SnMe$_3$) (Cp')L][Cp' = η^5-C_5H_5 (**4a**), η^5-C_5Me_5 (**4b**), η^5-C_9H_7 (**4c**)]

An excess of MgBrMe (0.60 mmol, 0.2 mL of 3 M solution in diethyl ether) was added to a suspension of 0.10 mmol of the corresponding trichlorostannyl complexes [Ru($SnCl_3$) (Cp')L] (**2a-c**) in 20 mL of diethyl ether cooled to −196 °C. The reaction mixture was allowed to reach room temperature and stirred for 6 h. The solvent was removed under vacuum, and the brown residue was dissolved in toluene (10 mL) and filtered through celite®. The solvent was removed under vacuum, and the brown residue was treated with ethanol (2 mL), affording a yellow product that was filtered, washed with ethanol (2 × 3 mL) and dried under reduced pressure.

(4a) Yield: 52%. Anal. Calc. for $C_{46}H_{46}O_2P_2RuSn$ (912.58): C, 60.54; H, 5.08. Found: C, 60.72; H, 5.19%. ^1H NMR (C_6H_6-d_6, 25 °C) δ: 8.10–6.80 (m, 30H, Ph), 5.72 (dd, $^3J_{H\text{-}P} = 13.2$ Hz, $^3J_{H\text{-}H} = 9.2$ Hz, 1H, C<u>H</u> L), 5.19 (cdd, $^3J_{H\text{-}P} = {}^3J_{H\text{-}H} = 9.2$ Hz, 1H, C<u>H</u> L), 4.70 (s, 5H, $C_5\underline{H}_5$), 0.63 (s, $^2J_{H\text{-}119Sn} = 35.2$ Hz, 9H, $SnMe_3$) ppm. $^{31}P\{^1H\}$ NMR (C_6H_6-d_6, 25 °C) δ: AB system, δ_A 164.5, δ_B 163.7 ($^2J_{AB} = 58.3$ Hz) ppm.$^{13}C\{^1H\}$ NMR (C_6H_6-d_6, 25 °C) δ: 151.1–127.4 (Ph), 85.4 (br t, $^2J_{C\text{-}P} = 3.0$ Hz, <u>C</u>H L), 82.8 (s, <u>C</u>H L), 82.4 (s, $\underline{C}_5H_5$), −1.4 (s, $J_{Sn\text{-}C} = 80.6$ Hz, $SnMe_3$) ppm. $^{119}Sn\{^1H\}$ NMR (C_6H_6-d_6, 25 °C) δ: 23.6 (cdd, $^2J^{119}_{Sn\text{–}P} \approx 260$ Hz) ppm. $[\alpha]_D^{24}$: −60.1 (*c* 0.10, Toluene).

(4b) Yield: 65%. Anal. Calc. for $C_{51}H_{56}O_2P_2RuSn$ (982.71): C, 62.33; H, 5.74. Found: C: 62.55; H: 5.80%. ^1H NMR (C_6H_6-d_6, 25 °C): δ 7.85–6.68 (m, 30H, Ph), 5.90 (dd, $^3J_{H\text{-}P} = 11.2$ Hz, $^3J_{H\text{-}H} = 7.9$ Hz, 1H, C<u>H</u> L), 4.98 (dd, $^3J_{H\text{-}P} = 9.7$ Hz, $^3J_{H\text{-}H} = 7.9$ Hz, 1H, C<u>H</u> L), 1.40 (s, 15H, $C_5\underline{Me}_5$), 0.30 (s, $^2J_{H\text{-}119Sn} \approx 17$ Hz, 9H, $SnMe_3$) ppm. $^{31}P\{^1H\}$ NMR (C_6H_6-d_6, 25 °C) δ: 172.2 (d, $^2J_{PP} = 59.7$ Hz, $^2J_{P\text{-}119Sn} = 293.5$ Hz, $^2J_{P\text{-}^{117}Sn} = 277.2$ Hz), 160.0 (d, $^2J_{PP} = 59.7$ Hz, $^2J_{P\text{-}^{119}Sn} = 293.8$ Hz, $^2J_{P\text{-}117Sn} = 282.5$ Hz) ppm. $^{13}C\{^1H\}$ NMR (C_6H_6-d_6, 25 °C): δ 147.1–127.3 (Ph), 93.7 (s, $\underline{C}_5Me_5$), 85.4 (d, $^2J_{C\text{-}P} = 10.1$ Hz, <u>C</u>H L), 83.3 (d, $^2J_{C\text{-}P} = 6.1$ Hz, <u>C</u>H L), 10.4 (s, $C_5\underline{Me}_5$), 1.4 (s, $J_{C\text{-}^{119}Sn} = 37.2$ Hz, $SnMe_3$) ppm. ^{119}Sn NMR (C_6H_6-d_6, 25 °C): δ 304.5 (cdd, $^2J^{119}_{Sn\text{–}P} \approx 292$ Hz) ppm. $[\alpha]_D^{24}$: 163.8 (c 0.20, Toluene).

(4c) Yield: 55%. Anal. Calc. for**:** $C_{50}H_{48}O_2P_2RuSn$ (962.64): C, 62.39; H, 5.03%. Found: C, 62.44; H, 5.20%. ^1H NMR (CH_2Cl_2-d_2, 25 °C) δ: 7.70–6.20 (m, 34H, Ph + $H_{5\text{-}7}$ ind.), 5.71 (s, 1H, H_2 C_9H_7), 5.05 (s, 1H, $H_{1,3}$ C_9H_7), 5.01 (dd, $^3J_{H\text{-}P} = 10.7$ Hz, $^3J_{H\text{-}H} = 7.8$ Hz, 1H, C<u>H</u> L), 4.64 (s, 1H, $H_{1,3}$ C_9H_7), 4.40 (dd, $^3J_{H\text{-}P} = 10.5$ Hz, $^3J_{H\text{-}H} = 7.8$ Hz, 1H, C<u>H</u> L), −0.09 (s, $^2J_{H\text{-}^{119}Sn} = 62.8$ Hz, $^2J_{H\text{-}^{117}Sn} = 19.04$ Hz, 9H, CH_3) ppm. $^{31}P\{^1H\}$ NMR (CH_2Cl_2-d_2, 25 °C) δ: AB system, δ_A 168.0 ($^2J_{P\text{-}^{119}Sn} = 290.0$ Hz, $^2J_{P\text{-}^{117}Sn} = 276.1$ Hz), δ_B 166.1 ($^2J_{P\text{-}^{119}Sn} = 207.0$ Hz, $^2J_{P\text{-}^{117}Sn} = 199.2$ Hz) ($^2J_{AB} = 56.5$ Hz) ppm. $^{13}C\{^1H\}$ NMR (CH_2Cl_2-d_2, 25 °C): δ 149.8–120.5 (Ph + $C_{5\text{-}8}$ C_9H_7), 113.1 (br s, $C_{4,9}$ C_9H_7), 106.4 (br s, $C_{4,9}$ C_9H_7), 91.5 (d, $^2J_{C\text{-}P} = 4.3$ Hz, C_2 C_9H_7), 84.8 (d, $^2J_{C\text{-}P} = 9.3$ Hz, <u>C</u>H L), 83.1 (d, $^2J_{C\text{-}P} = 6.6$ Hz, <u>C</u>H L), 70.7 (d, $^2J_{C\text{-}P} = 9.8$ Hz, $C_{1,3}$ C_9H_7), 67.3 (d, $^2J_{C\text{-}P} = 10.6$ Hz, $C_{1,3}$ C_9H_7), −2.0 (s, $J_{C\text{-}^{119}Sn} = 91.1$ Hz, CH_3) ppm. $^{119}Sn\{^1H\}$ NMR (CH_2Cl_2-d_2, 25 °C) δ: ABM system (M = ^{119}Sn) 48.6 ($^2J_{MA} = 290.0$ Hz, $^2J_{MB} = 207.0$ Hz) ppm. $[\alpha]_D^{27}$: 646.9 (c 0.23, $CHCl_3$).

4.3.5. [Ru{Sn(C≡CPh)$_3$}(Cp')L][Cp' = η^5-C_5H_5 (**5a**), η^5-C_5Me_5 (**5b**), η^5-C_9H_7 (**5c**)]

An excess of lithium phenylacetylide (1.70 mmol, 1.70 mL of a 1 M THF solution) was added to a suspension of 0.17 mmol of the corresponding trichlorostannyl complexes [Ru($SnCl_3$) (Cp')L] (**2a-c**) in 15 mL diethyl ether cooled to −196 °C. The mixture was warmed to room temperature and stirred for 3 h. The solvent was removed under vacuum, and the yellow residue was dissolved in toluene (20 mL) and filtered through celite®. The solvent was removed under vacuum affording an oil that was treated with ethanol (3 mL). The yellow solid obtained was filtered, washed with ethanol (2 × 3 mL) and dried under vacuum.

(5a) Yield: 65%. Anal. Calc. for $C_{67}H_{52}O_2P_2RuSn$ (1172.15): C, 68.59; H, 4.47. Found: C: 69.01; H: 4.52%. FT-IR (ATR): $\nu_{C\equiv C}$ 2124 (m) cm^{-1}.^1H NMR (CH_2Cl_2-d_2, 25 °C): δ 7.62–6.48 (m, 45H, Ph), 6.01 (dd, $^3J_{H\text{-}P} = 11.6$ Hz, $^3J_{H\text{-}H} = 8.2$ Hz, 1H, C<u>H</u> L), 4.93 (cdd, $^3J_{H\text{-}P} = {}^3J_{H\text{-}H} = 7.9$ Hz, 1H, C<u>H</u> L), 4.82 (s, 5H, C_5H_5) ppm. $^{31}P\{^1H\}$ NMR (CH_2Cl_2-d_2, 25 °C): δ AB, δ_A 162.7, δ_B 161.0, $^2J_{AB} = 59.0$ Hz ppm $^{13}C\{^1H\}$ NMR (CH_2Cl_2-d_2, 25 °C): δ 148.9–125.4 (Ph), 107.5 (s, C_β acetylide), 100.7 (s, C_α acetylide), 85.6 (d, $^2J_{C\text{-}P} = 9.1$ Hz, <u>C</u>H L), 83.6 (s, $\underline{C}_5H_5$), 82.9 (d, $^2J_{C\text{-}P} = 5.2$ Hz, <u>C</u>H L) ppm. $^{119}Sn\{^1H\}$ NMR (CH_2Cl_2-d_2, 25 °C): δ −248.5 (cdd, $^2J_{Sn\text{-}P} \approx 380$ Hz) ppm. $[\alpha]_D^{27}$: 245.4 (c 0.20, $CHCl_3$).

(5b) Yield: 60%. Anal. Calc. for $C_{72}H_{62}O_2P_2RuSn$ (1240.19): C, 69.69; H, 5.04. Found: C, 70.01; H, 5.01%. FT-IR (ATR): $\nu_{C\equiv C}$ 2127 (m) cm^{-1}.^1H NMR (CH_2Cl_2-d_2, 25 °C): δ 7.81–6.35 (m, 45H, Ph), 5.99 (dd, $^3J_{H\text{-}P} = 11.0$ Hz, $^3J_{H\text{-}H} = 8.5$ Hz, 1H, C<u>H</u> L), 4.72 (cdd, $^3J_{H\text{-}P} = {}^3J_{H\text{-}H} = 8.5$ Hz, 1H, C<u>H</u> L), 1.54 (s, 15H, $C_5\underline{Me}_5$) ppm. $^{31}P\{^1H\}$ NMR (CH_2Cl_2-d_2, 25 °C) δ: AB, δ_A 172.8 ($^2J_{P\text{-}^{119}Sn} = 369.6$ Hz, $^2J_{P\text{-}^{117}Sn} = 351.1$ Hz), δ_B 157.0 ($^2J_{P\text{-}^{119}Sn} = 395.7$ Hz, $^2J_{P\text{-}^{117}Sn} = 378.6$ Hz), $^2J_{AB} = 58.4$ Hz ppm $^{13}C\{^1H\}$ NMR (CH_2Cl_2-d_2, 25 °C): δ 146.4–125.7 (Ph), 107.2 (s, C_β acetylide), 103.3 (s, C_α acetylide), 93.1 (s, $\underline{C}_5Me_5$), 85.0 (d, $^2J_{C\text{-}P} = 10.0$ Hz, <u>C</u>H L), 83.2 (d, $^2J_{C\text{-}P} = 6.4$ Hz, <u>C</u>H L), 9.92 (s,

Table 5
Crystal data and structure refinement details for the **1b**, **2b** and **2c** compounds.

	1 b	2 b·2CHCl$_3$	2c·CHCl$_3$
Empirical formula	$C_{48}H_{47}ClO_2P_2Ru$	$C_{50}H_{49}Cl_9O_2P_2RuSn$	$C_{48}H_{40}Cl_6O_2P_2RuSn$
Formula weight	854.32	1282.64	1143.20
Temperature (K)	293 (2)	293 (2)	100 (2)
Wavelength (Å)	0.71073	0.71073	0.71073
Crystal system	Monoclinic	Tetragonal	Orthorhombic
Space group Unit cell dimensions	$P2_1$	$P4_1$	$P2_12_12_1$
a (Å)	17.28 (2)	15.3139 (5)	13.3511 (5)
b (Å)	11.666 (14)	15.3139 (5)	18.2904 (8)
c (Å)	20.74 (3)	23.1267 (10)	19.3411 (7)
β	102.21 (3)°	90°	90°
Volume (Å^3)	4086 (9)	5423.6 (3)	4723.0 (3)
Z	4	4	4
Density (calculated) (Mg/m^3)	1.389	1.571	1.608
Absorption coefficient (mm^{-1})	0.566	1.279	1.294
F (000)	1768	2568	2280
Crystal size (mm)	0.21 × 0.09 × 0.06	0.18 × 0.11 × 0.09	0.28 × 0.07 × 0.06
θ range for data collection (°)	2.24–26.47	2.58–28.32	2.38–28.33
Index ranges	$-21 \le h \le 19$ $-14 \le k \le 14$ $-25 \le l \le 25$	$-15 \le h \le 19$ $-20 \le k \le 13$ $-30 \le l \le 30$	$-17 \le h \le 17$ $-24 \le k \le 23$ $-25 \le l \le 25$
Reflections collected	57446	43324	42456
Independent reflections	16732 [R (int) = 0.0446]	13359 [R (int) = 0.0400]	11711 [R (int) = 0.0347]
Data completeness	0.995	0.999	0.996
Abs. Correc.	Semi-empirical from equivalents	Semi-empirical from equivalents	Semi-empirical from equivalents
Max. and min. transmission	0.7454 and 0.5166	0.7457 and 0.6182	0.9229 and 0.7093
Refinement method	Full-matrix least-squares on F2	Full-matrix least-squares on F2	Full-matrix least-squares on F2
Data/restraints/parameters	16732/1/960	13359/1/591	11711/0/541
Goodness-of-fit on F^2	0.686	1.022	1.033
Final R indices [I > 2σ(I)]	$R_1 = 0.0319$ $wR_2 = 0.0889$	$R_1 = 0.0399$ $wR_2 = 0.0776$	$R_1 = 0.0277$ $wR_2 = 0.0536$
R indices (all data)	$R_1 = 0.0378$ $wR_2 = 0.0963$	$R_1 = 0.0520$ $wR_2 = 0.0831$	$R_1 = 0.0333$ $wR_2 = 0.0555$
Absolute structure parameter	0.027 (15)	−0.030 (16)	−0.022 (13)
Largest diff. peak and hole, e.Å^{-3}	0.588 and −0.965	1.105 and −1.142	0.630 and −0.590

$C_5\underline{Me}_5$) ppm. $^{119}Sn\{^1H\}$ NMR (CH_2Cl_2-d_2, 25 °C): δ −233.2 (dd, $^2J^{119}_{Sn\text{-}PA=}$369.6 Hz, $^2J^{119}_{Sn\text{-}PB=}$395.0 Hz) ppm. $[\alpha]_D^{27}$: 134.5 (c 0.12, $CHCl_3$).

(5c) Yield: 70%. Anal. Calc. for $C_{71}H_{54}O_2P_2RuSn$ (1220.92): C, 69.85; H, 4.46. Found: C, 70.32; H, 4.21%. FT-IR (ATR): $\nu_{C\equiv C}$ 2125 (m) cm^{-1}.^{1}H NMR (CH_2Cl_2-d_2, 25 °C) δ: 7.51–6.21 (m, 49H, Ph + $H_{5\text{-}7}$ C_9H_7), 5.86 (s, 1H, H_2 C_9H_7), 5.72 (dd, $^3J_{H\text{-}P}$ = 11.4 Hz, $^3J_{H\text{-}H}$ = 8.0 Hz, 1H, C$\underline{H}$ L), 5.06 (s, 1H, $H_{1,3}$ C_9H_7), 5.03 (s, 1H, $H_{1,3}$ C_9H_7), 4.63 (cdd, $^3J_{H\text{-}P}$ = $^3J_{H\text{-}H}$ = 8.0 Hz, 1H, C$\underline{H}$ L) ppm. $^{31}P\{^1H\}$ NMR (CH_2Cl_2-d_2, 25 °C): δ AB, δ_A 166.6 ($^2J^{119}_{P\text{-}Sn}$ = 409.0 Hz, $^2J^{117}_{P\text{-}Sn}$ = 392.0 Hz), δ_B 162.7 ($^2J^{119}_{P\text{-}Sn}$ = 343.0 Hz, $^2J^{117}_{P\text{-}Sn}$ = 331.0 Hz) ($^2J_{AB}$ = 52.8 Hz) ppm. $^{13}C\{^1H\}$ NMR (CH_2Cl_2-d_2, 25 °C): δ 148.3–122.5 (Ph + $C_{5\text{-}8}$ C_9H_7), 109.0 (s, $C_{4,9}$ C_9H_7), 107.2 (s, C_β acetylide, $J^{119}_{C\text{-}Sn}$ = 51.3 Hz), 105.2 (s, $C_{4,9}$ C_9H_7), 99.6 (s, C_α acetylide, $J^{119}_{C\text{-}Sn}$ = 258.9 Hz), 92.7 (d, $^2J_{C\text{-}P}$ = 3.4 Hz, C_2 C_9H_7), 85.4 (d, $^2J_{C\text{-}P}$ = 9.5 Hz, C$\underline{H}$ L), 83.0 (d, $^2J_{C\text{-}P}$ = 6.0 Hz, C$\underline{H}$ L), 71.2 (d, $^2J_{C\text{-}P}$ = 5.8 Hz, $C_{1,3}$ C_9H_7), 69.7 (d, $^2J_{C\text{-}P}$ = 6.8 Hz, $C_{1,3}$ C_9H_7) ppm. $^{119}Sn\{^1H\}$ NMR (CH_2Cl_2-d_2, 25 °C): δ −267.0 (dd, $^2J^{119}_{Sn\text{-}PA}$ = 409.0 Hz, $^2J^{119}_{Sn\text{-}PB}$ = 343.0 Hz) ppm. $[\alpha]_D^{27}$: 425.5 (c 0.19, $CHCl_3$).

4.3.6. Crystal structure determination of [RuCl(η^5-C_5Me_5)L] (**1b**), [Ru($SnCl_3$)(η^5-C_5Me_5)L] (**2b**), and [Ru($SnCl_3$)(η^5-C_9H_7)L] (**2c**)]

Crystallographic data were collected on Bruker D8 Venture diffractometer at CACTI (Universidade de Vigo) with graphite monochromated Mo Kα radiation (λ = 0.71073 Å) and were corrected for Lorentz and polarization effects. APEX 3 software was used for collecting data frames, indexing reflections, and determining lattice parameters, SAINT [18] for integration of intensity of reflections and scaling, and SADABS [19] for empirical absorption correction. The crystallographic treatment of the compounds **1b**, **2b** and **2c** was performed with the SHELXL97 program [20]. The structures were solved by direct methods and refine by a full-matrix-least-squares based of F^2. Non-hydrogen atoms were refined with anisotropic displacement parameters. Hydrogen atoms were included in idealized positions and refined with isotropic displacement parameters. Details of crystal data and structural refinement are given in Table 5.

4.4. Computational details

DFT calculations were carried out with the Gaussian09 package [21]. X-Ray geometries were taken as starting points to perform DFT optimizations at the B3LYP/cc-pVDZ level. Heavy atoms, Ru and Sn, were described using the cc-pVDZ-PP basis set, which includes small-core relativistic pseudopotentials that account also for relativistic effects [9] Analytical vibrational frequency calculations were carried out to establish the minimum nature of each conformation. Later, NBO analysis [10] and calculation of Wiberg bond indices [11] were performed at the B3LYP6/cc-pVDZ (−PP) level.

Acknowledgements

Financial support from Xunta de Galicia (Spain) (research Project ED431D 2017/0) is gratefully acknowledged. We thank the Structural Determination Service of the Universidade de Vigo – CACTI for X-ray diffraction measurements and the collections of NMR data.

Appendix A. Supplementary data

Supplementary data related to this article can be found at https://doi.org/10.1016/j.jorganchem.2018.08.017.

References

[1] (a) X. Miao, A. Blokhin, A. Pasynskii, S. Nefedov, S.N. Osipov, T. Roisnel, C. Bruneau, P.H. Dixneuf, Organometallics 29 (2010) 5257–5262;
(b) M.P. Mingos, R.H. Crabtree (Eds.), Comprehensive Organometallic Chemistry, Elsevier, Amsterdam, 2007;
(c) W.R. Roper, L.J. Wright, Organometallics 25 (2006) 4704–4718;
(d) B. Eguillor, M. Esteruelas, M. Oliván, E. Oñate, Organometallics 24 (2005) 1428–1438;
(e) A.G. Davies, Organotin Chemistry, Wiley-VCH, Weinheim, Germany, 2004;
(f) F.G.A. Stone, E.W. Abel, G. Wilkinson (Eds.), Comprehensive Organometallic Chemistry, Pergamon Press, New York, 1995;
(g) M.F. Lappert, R.S. Rowe, Coord. Chem. Rev. 100 (1990) 267–292;
(h) M.S. Holt, W.L. Wilson, J.H. Nelson, Chem. Rev. 89 (1989) 11–49.

[2] (a) M. Novák, M. Bouška, L. Dostál, M. Lutter, K. Jurkschat, J. Turek, F. De Proft, Z. Růžičková, R. Jambor, Eur. J. Inorg. Chem. (2017) 1292–1300;
(b) G. Albertin, S. Antoniutti, J. Castro, S. Da Lio, Organometallics 32 (2013) 3651–3661;
(c) G. Albertin, S. Antoniutti, J. Castro, Organometallics 29 (2010) 3808–3816;
(d) G. Albertin, S. Antoniutti, S. García-Fontán, G. Zanardo, Organometallics 27 (2008) 2789–2794;
(e) G. Albertin, S. Antoniutti, A. Bacchi, G. Pelizzi, G. Zanardo, Organometallics 27 (2008) 4407–4418;
(f) G. Albertin, S. Antoniutti, J. Castro, S. García-Fontán, M. Noe, Dalton Trans. (2007) 5441–5452;
(g) H. Braunschweig, H. Bera, B. Geibel, R. Dörfler, D. Götz, F. Seeler, T. Kupfer, K. Radacki, Eur. J. Inorg. Chem. (2007) 3416–3424;
(h) M.M. Möhlen, C.E.F. Rickard, W.R. Roper, G.R. Whittell, L.J. Wright, Inorg. Chim. Acta. 360 (2007) 1287–1297;
(i) W.R. Roper, L.J. Wright, Organometallics 25 (2006) 4704–4718.

[3] (a) M.S. Winston, E.R. Batista, P. Yang, A.M. Tondreau, J.M. Boncella, Inorg. Chem. 55 (2016) 5534–5539.

[4] (a) P.A. Robles-Dutenhefner, E.M. Moura, G.J. Gama, H.G.L. Siebald, E.V. Gusevskaya, J. Mol. Catal. Chem. 164 (2000) 39–47;
(b) B.A.C. Silva, A.P. Guimaraes de Sousa, J.D. Ardinsson, H.G.L. Siebald, E. Moura, E.N. Santos, N.S. Mohallem, R. Montero Lago, Mater. Res. 6 (2003) 137–144.

[5] (a) A. Fuerte, M. Iglesias, F. Sánchez, J. Organomet. Chem. 588 (1999) 186–194;
(b) V.I. Tararov, R. Kadyrov, T.H. Riermeier, J. Holz, A. Börner, Tetrahedron Asymmetry 10 (1999) 4009–4015;
(c) G. Zhu, X. Zhang, J. Org. Chem. 63 (1998) 3133–3136;
(d) R.K. Sharma, A.G. Samuelson, Tetrahedron Asymmetry 18 (2007) 2387–2393;
(e) R.K. Sharma, M. Nethaji, A.G. Samuelson, Tetrahedron Asymmetry 19 (2008) 655–663.

[6] P. Bergamini, V. Bertolasi, M. Cattabriga, V. Ferretti, U. Loprieno, N. Mantovani, L. Marvelli, Eur. J. Inorg. Chem. (2003) 918–925.

[7] M. Kawashima, R. Hirata, Jpn. Kokai Tokkyo Koho (1994). JP 06345789 A 19941220.

[8] (a) R.P. Nair, K. Tae Ho, B.J. Frost, Organometallics 28 (2009) 4681–4688;
(b) M.I. Bruce, B.G. Ellis, B.W. Skelton, A.H. White, Organometallics 22 (2003) 3184–3198;
(c) I. De los Ríos, M. Jimenez Tenorio, J. Padilla, M.C. Puerta, P. Valerga, J. Chem. Soc., Dalton Trans. (1996) 377–381;
(d) J.R. Torres-Lubián, M.E. Sánchez-Castro, P. Juárez-Saavedra, J. Hernández-Martínez, B. Gordillo-Román, M.A. Paz-Sandoval, J. Organomet. Chem. 663 (2002) 127–133;
(e) S.A. Serron, L. Luo, E.D. Stevens, S.P. Nolan, Organometallics 15 (1996) 5209–5215;
(f) G. Consiglio, F. Morandini, G. Ciani, A. Sirone, M. Kretschmer, J. Am. Chem. Soc. 105 (1983) 1391–1392;
(g) E. Moura, H.G.L. Siebald, G.M. De Lima, Polyhedron 21 (2002) 2323–2331.

[9] (a) T.H. Dunning Jr., J. Chem. Phys. 90 (1989) 1007–1023;
(b) D.E. Woon, T.H. Dunning Jr., J. Chem. Phys. 98 (1993) 1358–1371;
(c) K.A. Peterson, J. Chem. Phys. 119 (2003) 11099–11112;
(d) K.A. Peterson, D. Figgen, M. Dolg, H. Stoll, J. Chem. Phys. 126 (2007), 124101-1 - 124101-12.

[10] (a) J.P. Foster, F. Weinhold, J. Am. Chem. Soc. 102 (1980) 7211–7218;
(b) F. Weinhold, J. Comput. Chem. 33 (2012) 2363–2379 (and references wherein);
(c) C.R. Landis, F. Weinhold, in: G. Frenking, S. Shaik (Eds.), The Chemical Bond: Fundamental Aspects of Chemical Bonding, Wiley-VCH, Weinheim, 2014.

[11] K.B. Wiberg, Tetrahedron 24 (1968) 1083–1096.

[12] A.E. Reed, R.B. Weinstock, F. Weinhold, J. Chem. Phys. 83 (1985) 735–746.

[13] (a) G. Chalasinski, M.M. Szczesniak, Chem. Rev. 100 (2000) 4227–4252;
(b) N. Kobko, J.J. Dannenberg, J. Phys. Chem. 105 (2001) 1944–1950.

[14] D.D. Perrin, W.L.F. Armarego, Purification of Laboratory Chemicals, third ed., Butterworth/Heinemann, London/Oxford, 1998.

[15] M.I. Bruce, C. Hameister, A.G. Swincer, R.C. Wallis, Inorg. Synth. 21 (1982) 78.

[16] M.S. Chinn, D.M. Heinekey, J. Am. Chem. Soc. 112 (1990) 5166–5175.

[17] L.A. Oro, M.A. Ciriano, M. Campo, C. Foces Foces, F.H. Cano, J. Organomet. Chem. 289 (1985) 117–131.

[18] SAINT Version 6.01, Data Integration Software Package, Bruker Analytical X-Ray Systems Inc., Madison, Wisconsin, USA, 1997.

[19] G.M. Sheldrick, SADABS. A Computer Program for Absorption Corrections, University of Göttingen, Germany, 1996.

[20] G.M. Sheldrick, Acta Crystallogr. A64 (2008) 112–122.

[21] M.J. Frisch, G.W. Trucks, H.B. Schlegel, G.E. Scuseria, M.A. Robb, J.R. Cheeseman, G. Scalmani, V. Barone, B. Mennucci, G.A. Petersson, H. Nakatsuji, M. Caricato, X. Li, H.P. Hratchian, A.F. Izmaylov, J. Bloino, G. Zheng, J.L. Sonnenberg, M. Hada, M. Ehara, K. Toyota, R. Fukuda, J. Hase - Gawa, M. Ishida, T. Nakajima, Y. Honda, O. Kitao, H. Nakai, T. Vreven, J.A. Montgomery Jr., J.E. Peralta, F. Ogliaro, M. Bearpark, J.J. Heyd, E. Broth-ers, K.N. Kudin, V.N. Staroverov, R. Kobayashi, J. Normand, K. Raghava-Chari, A. Rendell, J.C. Burant, S.S. Iyengar, J. Tomasi, M. Cossi, Rega, J.M. Millam, M. Klene, J.E. Knox, J.B. Cross, V. Bakken, C. Adamo, J. Jaramillo, R. Gomperts, R.E. Stratmann, O. Yazyev, A.J. Austin, R. Cammi, C. Pomelli, J.W. Ochterski, R.L. Martin, K. Morokuma, V.G. Zakrzewski, G.A. Voth, P. Salvador, J.J. Dannenberg, S. Dapprich, A.D. Daniels, O. Farkas, J.B. Foresman, J.V. Ortiz, J. Cioslowski, V. Fox, Gaussian 09, Revision A01, Gaussian, Inc., Wallingford, CT, USA, 2009.